Bioorganic Chemistry 93 (2019) 103328

Contents lists available at ScienceDirect

Bioorganic Chemistry

journal homepage: www.elsevier.com/locate/bioorg

New 4-*N*-phenylaminoquinoline derivatives as antioxidant, metal chelating and cholinesterase inhibitors for Alzheimer's disease

Rong Cai[a], Li-Ning Wang[b], Jing-Jing Fan[a], Shang-Qi Geng[a], Yu-Ming Liu[a,*]

[a] Department of Pharmacy Engineering, Tianjin University of Technology, Tianjin 300384, PR China
[b] College of Traditional Chinese Medicine, Tianjin Univerisity of Traditional Chinese Medicine, Tianjin 300193, PR China

ARTICLE INFO

Keywords:
Alzheimer's disease
Anti-cholinesterase activity
Antioxidant
Metal chelator
4-*N*-phenylaminoquinoline

ABSTRACT

A series of new 4-*N*-phenylaminoquinoline derivatives were designed, synthesized, and their anticholinesterase activities, 1,1-Diphenyl-2-picrylhydrazyl (DPPH) radical scavenging activity, metal-chelating ability were tested. Among them, compounds **11j**, **11k** and **11l** had comparable inhibition activities to reference drug galantamine both in AChE and in BChE. Especially, compound **11j** revealed the most potent inhibition to *ee*AChE and *eq*BChE with IC_{50} values of 1.20 μM and 18.52 μM, respectively. Furthermore, both kinetic analysis of AChE inhibition and molecular docking study indicated that compound **11j** was mixed-type inhibitor, binding simultaneously to the catalytic anionic site (CAS) and the peripheral anionic site (PAS) of AChE, and propidium iodide displacement assay showed significant displacement of propidium iodide with compound **11k** (25.80%) from PAS of *ee*AChE. More importantly, compound **11l** displayed excellent DPPH radical scavenging activity (84% at 1 mg/mL), and its EC_{50} value was 0.328 μM. In addition, compounds **11a**, **11j**, **11k** and **11l** exhibited obvious biometal chelating abilities toward Al^{3+}, Fe^{2+}, Cu^{2+} and Zn^{2+} ions. Taken together, 4-*N*-phenylaminoquinoline derivatives targeting multiple pathogenetic factors deserve further investigation for treatment of AD.

1. Introduction

Alzheimer's disease (AD) is one of the most common types of dementia, and has seriously threatened the health of old people. The illness progress is well-known by the advent of aphasia, apraxia, executive disorders, mood disturbances, and psychiatric symptoms [1,2]. The exact origin of AD is ambiguous [3] and combinatorial reasons such as genetic, lifestyle, and environmental factors are involved in the onset and progression of the disease [4]. Now, such cellular processes as neurotransmitter systems [5], excitotoxicity [6], beta-amyloid aggregation, abnormal tau phosphorylation [7], oxidative stress, metal ion deregulation and inflammation [8] have been considered as the main causes of AD. Though several novel therapeutic approaches were explored in the last few decades like apolipoprotein E, CREB signaling pathways, insulin resistance, etc. to identify the potential leads, but were unable to elicit significant clinical outcomes [6].

One therapeutic approach to enhance cholinergic neurotransmission is to increase acetylcholine (ACh) availability by inhibiting acetylcholinesterase (AChE) [9–13]. Thus far, several anti-AD drugs targeting AChEs have become available, including tacrine, donepezil, and the alkaloid galantamine. Compared with AChE, butyrylcholinesterase (BChE), the sister enzyme of AChE, plays a supportive role in the cholinergic neurotransmission. In the brain of healthy adults, AChE is very more active than BChE, and cause almost 80% ACh hydrolysis in the brain [14,15]. However, with the gradual severity of AD, AChE in the brain drops to 90% of the normal level, while the level of BChE is about doubled and tends to increase continuously [16]. And then the regulation of ACh is increasingly dependent on BChE in progressed AD [17–20]. Thus, the synergistic inhibition of both AChE and BChE enzymes may be one more valuable approach in the treatment of AD [21]. It is worth mentioning that AChE possesses two binding sites including the catalytic anionic site (CAS) and the peripheral anionic site (PAS). The new agents that serve as dual binding inhibitors for both CAS and PAS of AChE are more efficient in treating AD [22], as they can alleviate cognitive deficits by restoring cholinergic activity and prevent the deposition of beta-amyloid in the brain promoted by PAS of AChE [23]. As a result, novel AChE inhibitors targeting both CAS and PAS attract the attentions of medicinal chemists throughout the world.

Among the various causative factors involved in the pathogenesis of AD, oxidative stress has emerged as an important factor. Oxidative stress is caused by the imbalance of antioxidant defense system and intracellular reactive oxygen species (ROS) accumulation [24]. Unregulated reaction of molecular oxygen with the redox active metals can lead to the generation of ROS [25]. What's more, the excessive

* Corresponding author.
E-mail address: coumarin1968@hotmail.com (Y.-M. Liu).

https://doi.org/10.1016/j.bioorg.2019.103328
Received 14 July 2019; Received in revised form 26 September 2019; Accepted 27 September 2019
Available online 28 September 2019

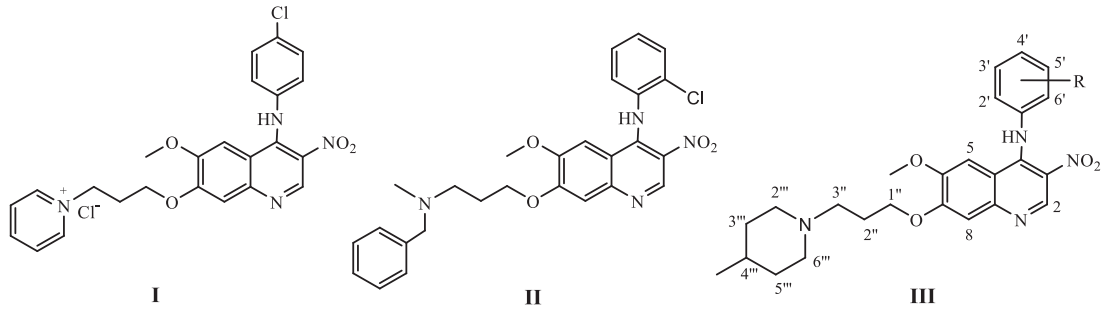

Fig. 1. Structures of previously reported compounds (**I**, **II**) and newly designed compounds **III**.

accumulation of metals promotes beta-amyloid fibril aggregates, which induce inflammation and activate neurotoxic pathways, leading to the dysfunction and death of brain cells [26,27]. Recent studies have shown that antioxidants can inhibit lipid peroxidation by acting as metal ion-chelating and free-radical scavenging agents [28]. Clinical studies have shown the particular therapeutic efficacy of several antioxidants. Therefore, antioxidation can be a key factor in AD treatment.

Quinoline derivatives are important compounds that exhibited various biological activities, such as anti-tumor, anti-malaria, and cholinesterase (ChE) inhibitory activity [29,30], and tacrine was before used as the first AChE inhibitor in the treatment of AD [31]. Recently some 4-*N*-phenylaminoquinoline analogues were synthesized and evaluated as AChE inhibitors [32–34]. The previous investigations in our laboratory had reported two lead structures derived from 4-*N*-phenylaminoquinoline – compounds **I** and **II** (Fig. 1). Compound **I** [16] was found to have more potent effects on inhibiting AChE and BChE (IC_{50} values equal to 0.92 μM and 14.20 μM, respectively) than galanthamine. Compound **II** [35] also showed significant inhibitory activities on AChE and BChE with IC_{50} values of 0.86 and 2.65 μM, respectively, a lot better than that of reference drug galanthamine. Furthermore, molecular modeling showed that compound **II** bind concomitantly to both catalytic and peripheral active site of AChE. As part of our ongoing project, we focused on their 4-*N*-phenylaminoquinoline core as a privileged skeleton for inhibiting AChE and BChE. On the other hand, a literature survey revealed that most of ChE inhibitors usually contain a tertiary amine unit in a ring or an open chain [36–39], which may play significant roles in the ChE inhibition. To this end, we employ molecular hybridization and bioisosterism replacement approaches to identify novel ChE inhibitors. Our design is based on bioisosteric replacement of *N*-methylbenzylamine moiety of compound **II** with 4-methylpiperidine fragment, with a lower structural weight and relatively small volume for improving brain exposure, to produce a class of compounds **III** (Fig. 1), which was inspired by this pharmacophoric unit with strong binding interactions to ChE [2,40,41].

Now in the present study, a series of new 4-*N*-phenylaminoquinoline derivatives (**11a–11m**) were designed, synthesized, and their anticholinesterase activities, 1,1-Diphenyl-2-picrylhydrazyl (DPPH) radical scavenging activity, metal-chelating ability were tested.

2. Results and discussion

2.1. Chemistry

According to scheme 1, compounds **11a–11m** were synthesized starting from the commercially available material vanillic acid, which was esterifcated with methanol under acidic conditions to obtain compound **2**. Compound **2** was alkylated with 1-bromo-3-chloropropane in acetone under basic condition to provide compound **3**, which was converted to nitro compound **4** using fuming nitric acid as nitration reagent in dichloromethane for **5**h with 98.98% yield. Compound **4** was reduced using iron powder and catalytic amounts of ammonium chloride in ethanol to obtain compound **5**, which was further hydrolyzed with NaOH to provide compound **6**. Next, intermediate **7** was formed by the reaction of compound **6** and 2-nitroacetaldoxime, which was prepared beforehand from nitromethane in the presence of NaOH. Compound **7** was cyclized with acetic anhydride to yield compound **8**, which was subsequently treated with phosphorus oxychloride to afford compound **9**. Compound **9** was further reacted with the corresponding aniline, affording compounds **10a–10m**. Then, final compounds **11a–11m** were achieved upon the substitution of compound **10a–10m** with excessive 4-methyl-piperidine, respectively. All target compounds were purified by column chromatography and characterized by ^{1}H NMR, ^{13}C NMR, and HR-ESI-MS.

2.2. Biological evaluation

2.2.1. AChE and BChE inhibition assay

All synthesized quinoline derivatives (**11a–11m**) were evaluated for their ChE inhibitory activities on electric eel acetylcholinesterase (*ee*AChE) and equine serum butyrylcholinesterase (*eq*BChE), by the Ellman's method with galanthamine as the reference drug. The results showed that most 4-*N*-phenylaminoquinoline derivatives have inhibitory effects on AChE. Compared with compounds **11k** and **11l**, compounds **11e**, **11f** and **11g** had relatively weaker inhibitory activities. It seems that AChE inhibitory activities can be enhanced when there is electron-donating group (such as hydroxyl) in 4-*N*-substituted aniline ring, and that relative activities are reduced when electron-withdrawing group is present (such as chlorine atom).

As shown in Table 1, what exhibited more potent on AChE than galanthamine were compound **11j** with a *para* methoxy group (IC_{50} = 1.20 μM) and compound **11k** with a *meta* hydroxyl group (IC_{50} = 1.23 μM). According to the different substituents, the order of the inhibitory potency of these derivatives bearing different *o*-substituted groups was hydrogen atom > chloro group > methoxy group > methyl group; the order with different *m*-substituted groups was as followed: hydroxyl group > hydrogen atom > chloro group > methyl group > methoxy group > trifluoromethyl group; and the order with different *p*-substituted groups was: methoxy group > hydrogen atom > hydroxyl group > methyl group > chloro group. On the other hand, based on the substituted position in the 4-*N*-substituted aniline ring, the order of inhibitory potency against AChE was: Meta > Ortho > Para, but it turned to be: Para > Meta > Ortho after methoxyl substitution. Therefore, their anti-AChE activities directly depended on the electronic properties and position of different substituents on the aniline ring.

In terms of inhibitory activity against *eq*BChE, although the activities of compounds **11a–11 g**, **11m** were weak, compounds **11j**, **11k**, **11l** showed considerable activities. And compared with compound **11a**, compounds with hydroxyl or methoxy group (i.e., compounds **11h–11l**) were more favorable to the inhibitory activity. Interestingly, the position of methoxy substitution on phenyl ring has an essential effect on inhibiting BChE. When the methoxy group was shifted from 2-position or 3-position to 4-positon of the phenyl ring, almost a 3-fold improvement in BChE inhibition was observed, and the obtained compound **11j**

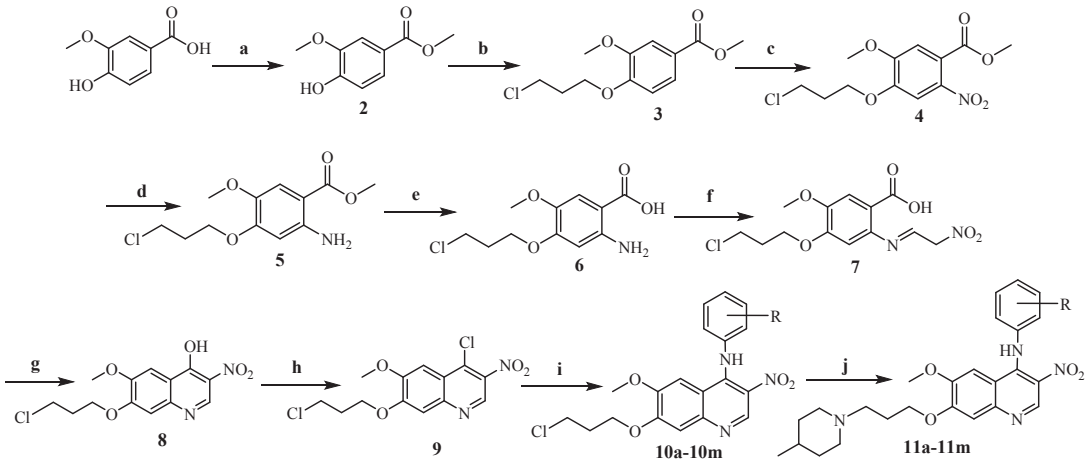

Scheme 1. Synthesis of compounds **11a–11m**. Reagents and conditions: (a) MeOH, HCl, 70 °C, 10 h (94.36%); (b) $Br(CH_2)_3Cl$, K_2CO_3, acetone, 70 °C, 10 h (92.85%); (c) fuming HNO_3, CH_2Cl_2, room temperature, 5 h (98.98%); (d) Fe, NH_4Cl, EtOH, reflux (66.67%); (e) 5% NaOH, EtOH, 50 °C, 10 h (80.68%); (f) HON = $CHCH_2NO_2$, HCl, room temperature, 18 h (87.97%); (g) KOAc, Ac_2O, 15 min, reflux (32.24%); (h) $POCl_3$, 70 °C, 10 h (87.29%); (i) corresponding aniline, isopropanol, 90 °C, 12 h (80.65% − 95.63%); (j) 4-methyl-piperidine, NaI, K_2CO_3, CH_3CN, 87 °C, 24 h, reflux (43.36 − 56.79%).

Table 1
Inhibition of cholinesterases activity and selectivity index (SI) of compounds **11a–11m**.

Compd.	R	*ee*AChE IC_{50} (μM)[a]	*eq*BChE IC_{50} (μM)[a]	SI[b]
11a	H	1.35 ± 1.20	> 150	> 111.11
11b	2-CH_3	3.03 ± 1.34	> 150	> 49.50
11c	3-CH_3	1.65 ± 0.64	> 150	> 90.90
11d	4-CH_3	12.34 ± 3.00	142.40 ± 3.95	11.51
11e	2-Cl	1.81 ± 0.60	121.44 ± 1.52	67.09
11f	3-Cl	1.54 ± 0.50	126.67 ± 5.84	82.25
11g	4-Cl	14.05 ± 0.03	> 150	> 10.67
11h	2-OCH_3	2.32 ± 0.03	52.29 ± 2.81	22.54
11i	3-OCH_3	1.70 ± 0.08	53.88 ± 1.68	31.69
11j	4-OCH_3	1.20 ± 0.18	18.52 ± 1.21	15.43
11k	3-OH	1.23 ± 0.03	22.11 ± 1.43	17.98
11l	4-OH	1.40 ± 0.23	28.43 ± 4.70	20.31
11m	3-CF_3	2.95 ± 0.57	102.17 ± 3.23	34.63
Galanthamine		1.28 ± 0.01	24.41 ± 2.01	19.07

[a] IC_{50} values are at least from three independent experiments and are expressed as the means ± SD.
[b] SI for AChE = IC_{50} *eq*BChE/IC_{50} *ee*AChE.

(IC_{50} = 18.52 μM) presented the most potent BChE inhibitory activity in this series.

Taken as a whole, all SI values are greater than 10, so the activity characteristics of all compounds is that their inhibitory activities on AChE are stronger than on BChE. It's worth mentioning that the SI value of compounds **11a–11c**, **11e, 11f** are all over 40, indicating that these compounds possess rather high selectivity to AChE.

2.2.2. Enzyme kinetic analysis against AChE

The kinetics of more active compounds (**11a**, **11j**, **11k**, **11l**) was further studied to understand the nature of AChE inhibition. The results from Fig. 2 exhibited that all of the compounds (**11a**, **11j**, **11k**, **11l**) are reversible inhibitors, as in the presence of different concentrations of compounds, plots of the initial velocity versus enzyme concentration gave a series of straight lines, all of which passed through the origin.

The kinetic characterization of four active compounds (**11a**, **11j**, **11k**, **11l**) against *ee*AChE was also studied to elucidate the inhibition type and inhibition constant. The analysis was carried out by measuring enzyme's activity at different concentrations of substrate (0.5 μM–2.0 μM). The acquired inhibition data were further depicted with Lineweaver-Burk method followed by inhibition constant (K_i) calculation using Lineweaver-Burk secondary plot. Results in Fig. 3 showed that compounds **11a**, **11j** and **11k** had a family of lines with a common intercept on the left of the vertical axis and above the horizontal axis, except compound **11l** which lines were below the horizontal axis. All of these lines had no intersection on the horizontal or vertical axis, indicating that compounds **11a**, **11j**, **11k** and **11l** cause a mixed type of inhibition. This pattern of inhibition is usually the result of a combination of partially competitive and non-competitive inhibitions [42]. Then the inhibition constants K_i for compounds **11a**, **11j**, **11k** and **11l** were calculated as 0.46 μM, 0.14 μM, 0.40 μM and 1.47 μM, respectively.

2.2.3. Propidium iodide displacement assay

Propidium iodide assay is used to determine the displacement of propidium iodide (a selective PAS-AChE inhibitor) from the propidium iodide-AChE enzyme complex. The results obtained in Table 2 showed that compound **11k** was more efficient to displace propidium (25.80%) than donepezil (18.50%), although compounds **11j** and **11l** appeared to be somewhat less potent (13.78–14.85%), with the exception of **11a**, which only showed about half of displacement capability of donepezil.

2.2.4. DPPH radical scavenging activity

As ROS support the development and progression of AD [43], the antioxidant activity of four active compounds (**11a**, **11j**, **11k**, **11l**) were evaluated by the DPPH test [44]. The result indicated that the radical scavenging activity of compound **11l** increased with increasing of its concentration. However, compound **11j** didn't exhibit the similar capability, and even the percentage change of compounds **11a** and **11k** in scavenging activity was decreased with negative values. As is shown in Fig. 4, radical scavenging activity of ascorbic acid (Vc), as standard antioxidant, increased from 31% (at 0.0625 mg/mL) to 91% (at 0.25 mg/mL), and reached the maximum of 97% (at 1 mg/mL). The sharp increase appeared relatively late for the activity of compound **11l**, from 36% (at 0.25 mg/mL) doubled to 78% (at 0.5 mg/mL), and finally reached a maximum of 84% (at 1 mg/mL), only 13% lower than Vc. Nevertheless, when the concentration increased to 0.5 mg/mL, the radical scavenging activity of compound **11l** was basically stable and quite close to Vc. And the lower EC_{50} value (0.328 μM) of compound **11l** manifests its remarkable antioxidant effect, which was in submicromolar range similarly to Vc (EC_{50} = 0.095 μM).

2.2.5. Metal-chelating properties

The ability of the synthesized compounds in metal chelation would be an added advantage in the treatment of AD. Herein, compounds **11a**,

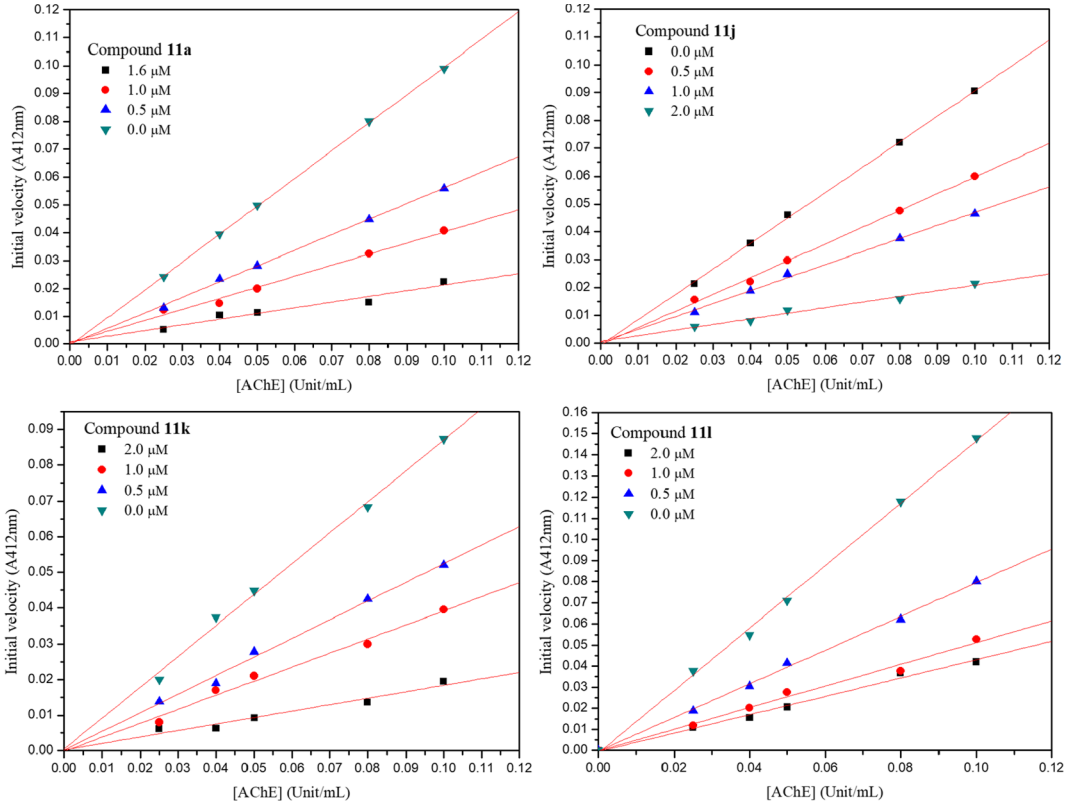

Fig. 2. Plots of initial velocity versus enzyme concentration for the inhibition of compounds **11a**, **11j**, **11k** and **11l** (0.025 U/mL, 0.04 U/mL, 0.05 U/mL, 0.08 U/mL, 0.10 U/mL) on the hydrolysis activity of *ee*AChE.

11j, **11k** and **11l** were selected for their chelating abilities toward Cu^{2+}, Fe^{2+}, Al^{3+} and Zn^{2+}, using UV spectrophotometer with wavelength ranging from 200 nm to 600 nm. As is seen in Fig. 5, the spectrum of compound **11l** changed significantly by adding $CuCl_2$. The maximum absorption at 308 nm shifted to 282 nm, and the blue shift was 26 nm, which indicated the formation of **11l**-Cu^{2+} complex. In addition, the absorption decreased significantly when $AlCl_3$, $FeCl_2$, and $ZnCl_2$ were added, indicating a possible interaction between the compound **11l** and these biometals. However, no remarkable shifts were observed upon the addition of $AlCl_3$, $FeCl_2$ or $ZnCl_2$. Similarly, the dramatic decreases in absorbance indicated a possible interaction between these biometals and compounds **11a**, **11j** and **11k**, which suggested that all compounds **11a**, **11j** and **11k** are also able to chelate biometals. The chelating ability of compound **11l** towards Cu^{2+} could be due to the donation of lone pair of electron on the nitrogen atom present in 4-*N*-substituted aniline ring, which might be easily stabilised by resonance through the phenol-quinone tautomerization, and strongly interfere in conjugated system between 4-*N*-substituted aniline ring and quinoline ring leading to a relative blue shift.

To further determine the stoichiometry of **11l**-Cu^{2+} complex, molar ratio method was used by preparing the methanol solutions of compound **11l** with increasing amounts of $CuCl_2$. The UV spectra were used to obtain the absorbance of the **11l** complex and different concentrations of $CuCl_2$ at 282 nm (Fig. 6). Accordingly, the absorbance linearly decreased initially and then plateaued. The two straight lines intersected at a mole fraction of 0.50, revealing a 2:1 stoichiometry for **11l**-Cu^{2+} complex.

2.3. Docking studies

In order to explore the possible interaction mode in the active sites of AChE, the most active compound **11j** was selected for molecular modeling research using CDOCKER in Discovery Studio 3.0 software. The crystal complex of AChE with galanthamine (PDB: 1DX6) was selected for the docking research [35]. Fig. 7 showed that compound **11j** interacted with the CAS site of AChE by the following moieties: the propyl ether fragment attached to quinoline nucleus showed one carbon hydrogen bond with His440; 4-*N*-phenylamine fragment created one π-π interaction with Phe331; 4-methyl-piperidine fragment of compound **11j** formed one π-alkyl interaction and one carbon hydrogen bond concurrently with Trp84. It is worth mentioning that there are three amino acids of PAS site of AChE binding to compound **11j**: Asp72 interacted with nitro group through one attractive charge, and with C-2 hydrogen through one carbon hydrogen bond; Tyr334 interacted with 4-*N*-phenylaminoquinoline skeleton through two π-π interactions; and Tyr121 interacted with the NH group via one conventional hydrogen bond. The binding mode suggests that compound **11j** behaves as dual binding site AChE inhibitors, which is consistent with our kinetic analysis.

Noteworthily, nitrogen cation of the nitro group could form the attractive force with carboxyl anion of Asp72, an ion of opposite charge. And the strong electron-withdrawing ability of the nitro group could decrease the electron density of quinoline ring, and induces face-to-face π-π electron-donor-acceptor interaction with the aromatic amino acid residue (Tyr334) of AChE. Furthermore, other relative reports also suggested its important role in the AChE inhibition [45,46]. Unexpectedly, it was found from recent literatures that the nitro substituent of aromatic compounds could cause surprisingly monoamine oxidase (MAO) inhibitory and *N*-methyl-D-aspartate (NMDA) antagonistic effects [47,48]. So, the presence of nitro group might represent a valuable pharmacophoric feature for the treatment of AD.

The interaction of compound **11j** with BChE (PDB code: 4BDS) was also carried out. As seen in Fig. 8, compound **11j** was bound to the residues Gly117 and Gly116 from the oxyanion hole (OAH), Ser198 from esteratic site (ES), Trp82 from anionic substrate binding site (AS), three PAS amino acid residues such as Asp70, Pro285 and Tyr332, but

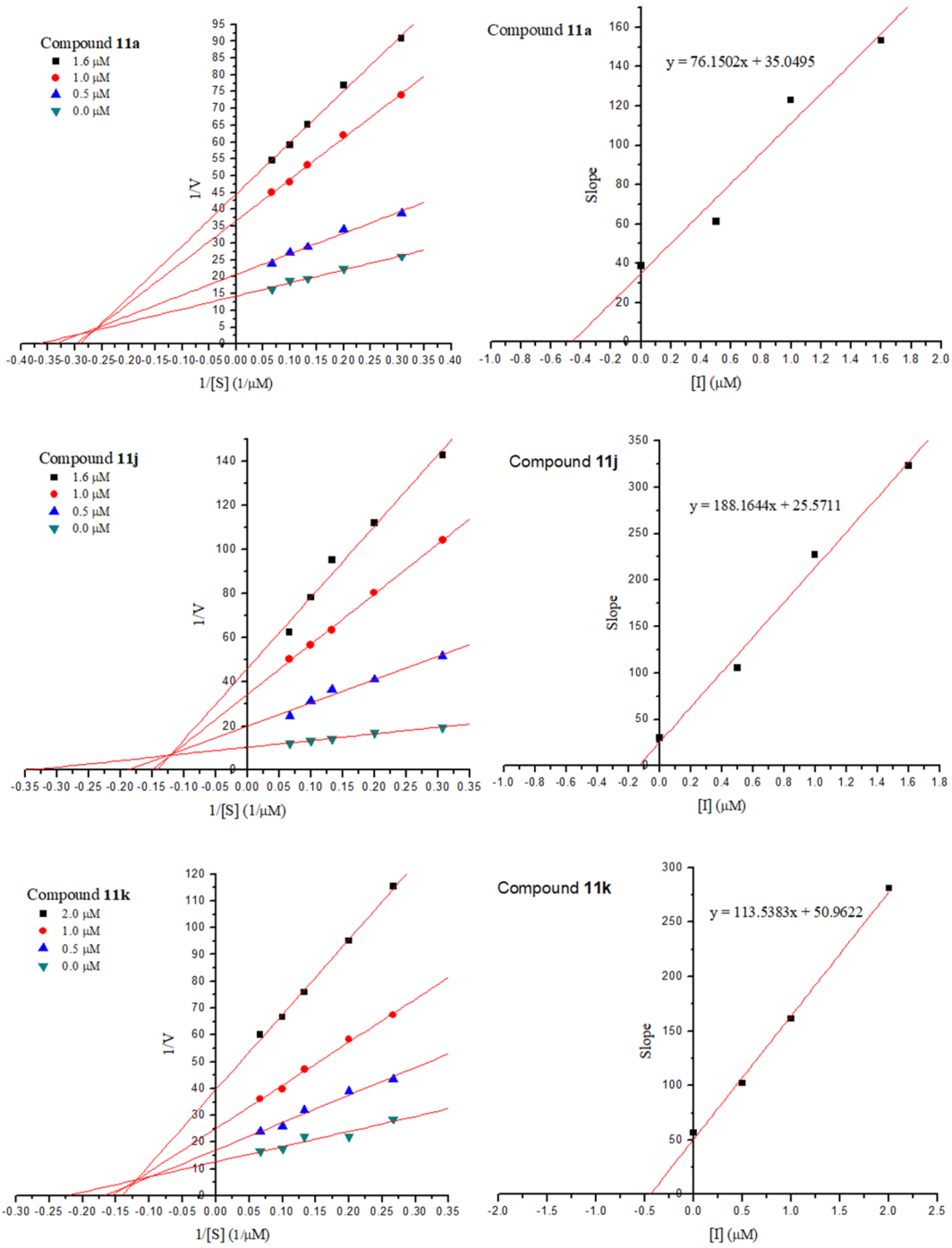

Fig. 3. *Left:* Lineweaver-Burk plots for the inhibition of *ee*AChE by compounds **11a**, **11j**, **11k** and **11l** at different concentrations of substrate (ATCh), *Right:* Secondary plots for calculation of steady-state inhibition constants (K_i) of compounds **11a**, **11j**, **11k** and **11l**.

also bound to Leu286, Ser287, Trp231 and Thr120 residues, via two π-ion interactions, two conventional hydrogen bond, four carbon hydrogen bonds, two amide-π interactions, one π-sigma interaction, one van der Waals, and two hydrophobic interactions. Briefly, it is noteworthy to say that compound **11j** interacted with important amino acid residues in the OAH, ES, AS and PAS active sites of BChE, which makes it worthy of further study.

3. Conclusion

In summary, a series of novel 4-*N*-phenylaminoquinoline derivatives were designed, synthesized and evaluated as multifunctional agents for the treatment of AD. Among them, compounds **11j**, **11k** and **11l** had comparable inhibition activities to galantamine in both AChE and BChE. Especially, compound **11j** demonstrated the most potent inhibition to *ee*AChE and *eq*BChE with IC_{50} values of 1.20 μM and 18.52 μM, respectively. The kinetic analysis inferred that compound **11j** was reversible inhibitor, and showed a mixed type of inhibition on AChE. What's more, through molecular docking studies, it was found that compound **11j** interacted with CAS and PAS of both AChE and BChE. Meanwhile, compound **11k** exhibited significant displacement of propidium iodide from the PAS of AChE (25.80%). More importantly, The DPPH radical scavenging activity of compound **11l** reached 84% (at 1 mg/mL), and its EC_{50} value of compound **11l** was 0.328 μM, which

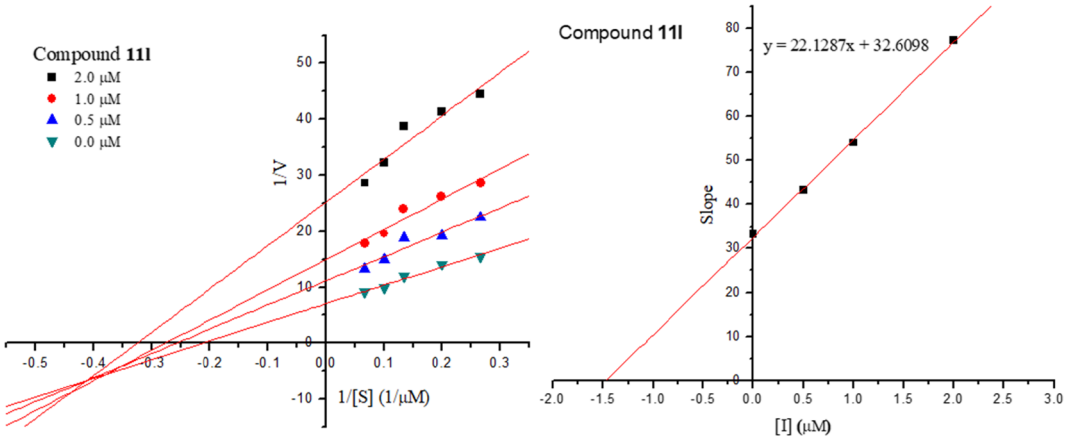

Fig. 3. (*continued*)

Table 2
Propidium iodide displacement (*ee*AChE) assay.

Compd.	Propidium iodide displacement (%)[a]
11a	9.73 ± 0.62
11j	14.85 ± 0.59
11k	25.80 ± 1.37
11l	13.78 ± 0.96
Donepezil	18.50 ± 1.13

[a] All values are expressed as the mean ± SD (n = 3).

was almost as high level as that of Vc (EC_{50} = 0.095 μM). Additionally, compounds **11a**, **11j**, **11k** and **11l** showed satisfactory metal-chelating properties toward Al^{3+}, Fe^{2+}, Cu^{2+} and Zn^{2+} ions. From our in vitro and in silico results, 4-*N*-phenylaminoquinoline might be a multi-functional potential scaffold for the treatment of AD, and compounds **11j**, **11k** and **11l** could provide a starting point for further developments of new therapeutic agents.

4. Experimental section

4.1. Chemistry

The chemical reactions were monitored by TLC using commercially available alumina plates coated with silica gel 60 F254 (Merck). Chromatographic separation was performed on self-packed columns with silica gel from Qingdao Haiyang Chemical Group Co., Ltd. (PR China), and MPLC was carried out on a BUCHI apparatus equipped with a C-605 pump. ^{1}H and ^{13}C NMR spectra were recorded on a Bruker Avance III 400 spectrometer with TMS as an internal standard. Coupling constant (*J*) values were presented in Hz, and spin multiplicities were given as s (singlet), d (doublet), t (triplet), q (quartet), brs (broad) and m (multiplet). The purity of all compounds for biological evaluation was confirmed to be higher than 95% by analytical HPLC performed on Shimadzu SPD-M20A (Column: WondaSil C18, 5 μm particle size, 4.6 mm × 250 mm, S/N: 3k9701-01; mobile phase: methanol/H_2O (30/70–100/0); flow rate = 1 mL/min; λ = 308 nm). High-resolution electrospray ionization mass spectrometry (HR-ESI-MS) was acquired on a Bruker micrOTOF-Q II spectrometer.

Compounds **2–9**, **10a–10m** were synthesized as our early reported procedures [16,35].

4.1.1. Synthesis of 6-Methoxy-7-(3-(4-methylpiperidin-1-yl)propoxy)-3-nitro-N-phenylquinolin-4-amine derivatives (11a–11m)

A mixture of 6-Methoxy-7-(3-chloropropoxy)-3-nitro-*N*-phenylquinolin-4-amine (**10a–10m**) (0.59 mmol), NaI (0.098 g, 0.65 mmol), K_2CO_3 (0.013 g, 1.77 mmol) was refluxed in CH_3CN (45 mL) for 1 h, then added 4-methyl-piperidine (0.71 mmol) refluxed for 24 h. Excess CH_3CN was rotated off, and the residue was partitioned between CH_2Cl_2 and H_2O and filtered through Celite. The organic portion was worked up to give a solid which was chromatographed on silica gel. CH_2Cl_2/MeOH (9:2) eluted products **11a–11m.**

4.1.2. 6-Methoxy-7-(3-(4-methylpiperidin-1-yl)propoxy)-3-nitro-N-phenylquinolin-4-amine (11a)

Yield: 46.78%, yellow solid, mp: 177.8–180.3 °C. Purity 95.65% by HPLC. ^{1}H NMR (400 MHz, $CDCl_3$) *δ*: 0.93 (d, 3H, *J* = 6.3 Hz, CH_3), 1.26 (m, 2H, H-3‴$_{ax}$ and H-5‴$_{ax}$), 1.35 (m, 1H, CH), 1.63 (d, 2H, *J* = 12.4 Hz, H-3‴$_{eq}$ and H-5‴$_{eq}$), 1.95 (t, 2H, *J* = 11.4 Hz, H-2‴$_{ax}$ and 6‴$_{ax}$), 2.10 (m, 2H, CH_2**CH_2**CH_2), 2.52 (t, 2H, *J* = 7.1 Hz, NCH_2), 2.91 (d, 2H, *J* = 11.4 Hz, H-2‴$_{eq}$ and H-6‴$_{eq}$), 3.34 (s, 3H, OCH_3), 4.23 (t, 2H, *J* = 6.6 Hz, OCH_2), 6.88 (s, 1H, H-5), 7.19 (d, 2H, *J* = 7.7 Hz, H-2′, H-6′), 7.25 (t, 1H, *J* = 7.7 Hz, H-4′), 7.35 (s, 1H, H-8), 7.41 (t, 2H, *J* = 7.7 Hz, H-3′, H-5′,), 9.36 (s, 1H, H-2), 10.43 (s, 1H, NH); ^{13}C NMR (100 MHz, $CDCl_3$) *δ*: 153.7, 148.3, 148.1, 145.2, 145.0, 141.2, 129.7 (2C), 128.5, 126.0, 124.0 (2C), 112.6, 109.9, 106.4, 67.8, 55.3, 55.2,

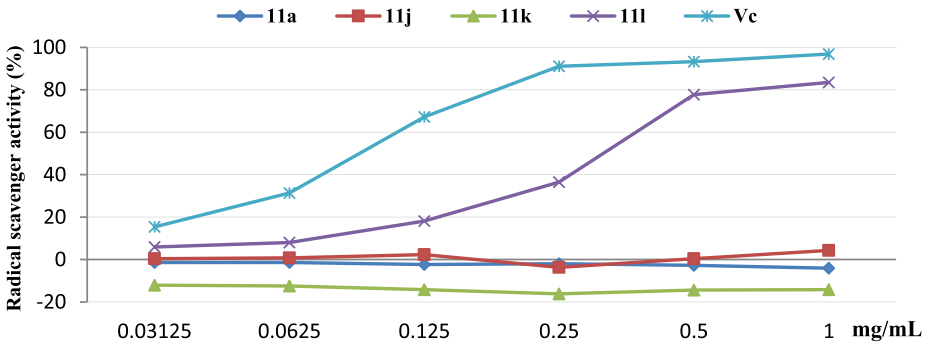

Fig. 4. Free radical scavenging activities of compounds **11a, 11j, 11k, 11l** and Vc.

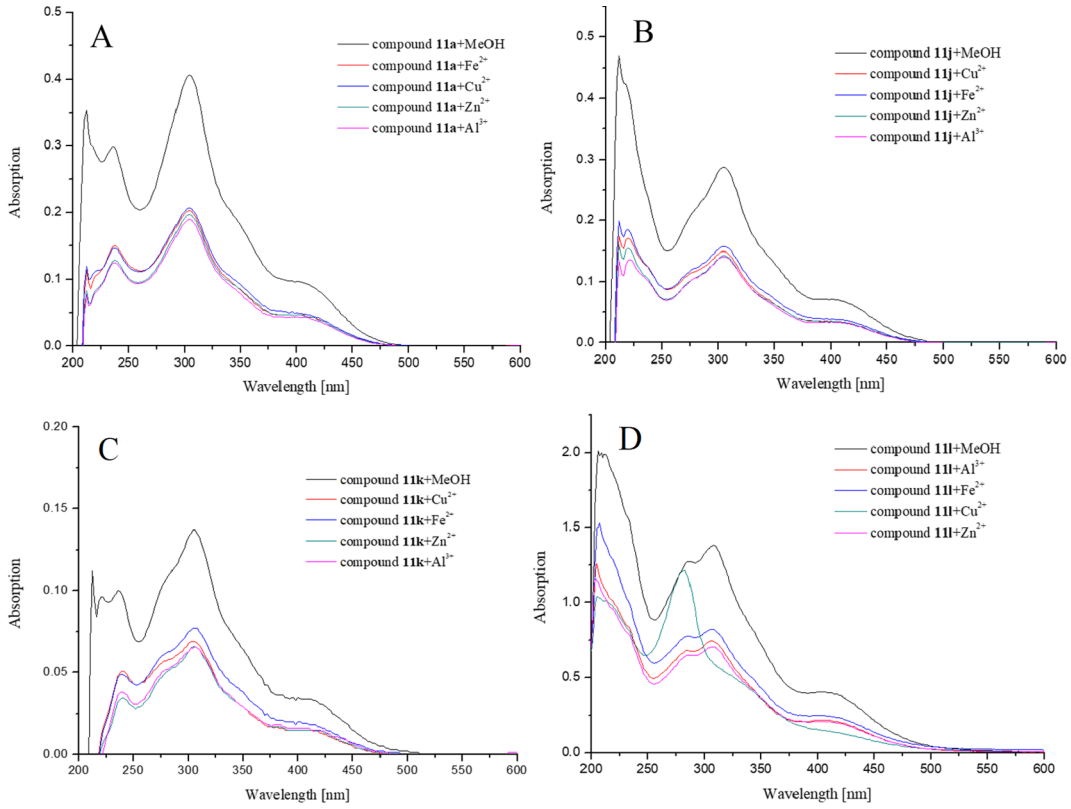

Fig. 5. UV–vis absorption spectra of test compound (20 μM in methanol) alone or in the presence of $AlCl_3$, $FeCl_2$, $CuCl_2$ or $ZnCl_2$ (20 μM, in methanol); (A) compound **11a**, (B) compound **11j**, (C) compound **11k**, (D) compound **11l**.

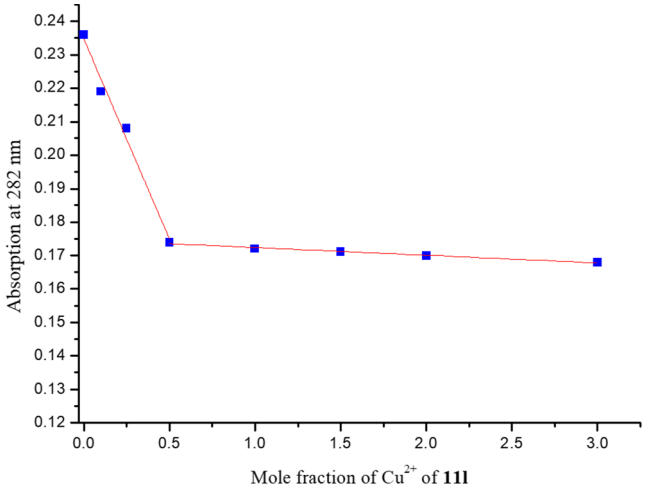

Fig. 6. Determination of the stoichiometry of complex **11l**-Cu^{2+} by using molar ratio method through titrating methanol solution of compound **11l** with ascending amounts of $CuCl_2$.

54.0 (2C), 34.3(2C), 30.8, 26.5, 21.9. HRMS (ESI) calculated for ($C_{25}H_{30}N_4O_4$ + H^+) 451.2345, found 451.2351.

*4.1.3. 6-Methoxy-7-(3-(4-methylpiperidin-1-yl)propoxy)-3-nitro-N-(o-tolyl)quinolin-4-amine (**11b**)*

Yield: 43.36%, yellow solid, mp: 166.6–168.9 °C. Purity 99.85% by HPLC. ^{1}H NMR (400 MHz, $CDCl_3$) δ: 0.92 (d, 3H, J = 6.3 Hz, CH_3), 1.25 (m, 2H, H-3‴$_{ax}$ and H-5‴$_{ax}$), 1.35 (m, 1H, CH), 1.62 (d, 2H, J = 12.6 Hz, H-3‴$_{eq}$ and H-5‴$_{eq}$), 1.93 (t, 2H, J = 11.4 Hz, H-2‴$_{ax}$ and 6‴$_{ax}$), 2.08 (m, 2H, CH_2**CH_2**CH_2), 2.35 (s, 3H, $ArCH_3$), 2.50 (t, 2H, J = 7.0 Hz, NCH_2), 2.89 (d, 2H, J = 11.4 Hz, H-2‴$_{eq}$ and H-6‴$_{eq}$), 3.27 (s, 3H, OCH_3), 4.21 (t, 2H, J = 6.6 Hz, OCH_2), 6.77 (s, 1H, H-5), 7.10 (m, 1H, ArH), 7.23 (m, 2H, ArH), 7.33 (s, 1H, H-8), 7.37 (m, 1H, ArH), 9.36 (s, 1H, H-2), 10.52 (s, 1H, NH); ^{13}C NMR (100 MHz, $CDCl_3$) δ: 153.5, 148.3, 147.8, 146.1, 145.6, 139.6, 133.5, 131.4, 127.3, 127.2, 127.1, 125.7, 112.4, 110.0, 105.5, 67.8, 55.3, 55.1, 54.0 (2C), 34.3 (2C), 30.8, 26.5, 21.9, 18.3. HRMS (ESI) calculated for ($C_{26}H_{32}N_4O_4$ + H^+) 465.2502, found 465.2516.

*4.1.4. 6-Methoxy-7-(3-(4-methylpiperidin-1-yl)propoxy)-3-nitro-N-(m-tolyl)quinolin-4-amine (**11c**)*

Yield: 48.29%, yellow solid, mp: 120.0–122.3 °C. Purity 96.39% by HPLC. ^{1}H NMR (400 MHz, $CDCl_3$) δ: 0.94 (d, 3H, J = 5.9 Hz, CH_3), 1.37 (m, 2H, H-3‴$_{ax}$ and H-5‴$_{ax}$), 1.42 (m, 1H, CH), 1.67 (d, 2H, J = 11.3 Hz, H-3‴$_{eq}$ and H-5‴$_{eq}$), 2.07 (t, 2H, J = 11.5 Hz, H-2‴$_{ax}$ and 6‴$_{ax}$), 2.16 (m, 2H, CH_2**CH_2**CH_2), 2.34 (s, 3H, $ArCH_3$), 2.62 (t, 2H, J = 7.6 Hz, NCH_2), 3.00 (d, 2H, J = 11.5 Hz, H-2‴$_{eq}$ and H-6‴$_{eq}$), 3.34 (s, 3H, OCH_3), 4.22 (t, J = 6.5 Hz, 2H, OCH_2), 6.90 (s, 1H, H-5), 6.98 (d, J = 8.0 Hz, 1H, H-4′), 7.01 (s, 1H, H-2′), 7.06 (d, 1H, J = 7.5 Hz, H-6′), 7.28 (t, 1H, J = 7.7 Hz, H-5′), 7.32 (s, 1H, H-8), 9.32 (s, 1H, H-2), 10.42 (s, 1H, NH); ^{13}C NMR (100 MHz, $CDCl_3$) δ: 153.3, 148.2, 147.9, 145.3, 145.1, 141.0, 139.9, 129.5, 128.4, 126.9, 124.7, 121.2, 112.9, 110.0, 106.6, 67.3, 55.2, 55.1, 53.6 (2C), 33.1 (2C), 31.8, 25.6, 21.4, 21.3. HRMS (ESI) calculated for ($C_{26}H_{32}N_4O_4$ + H^+) 465.2502, found 465.2510.

*4.1.5. 6-Methoxy-7-(3-(4-methylpiperidin-1-yl)propoxy)-3-nitro-N-(p-tolyl)quinolin-4-amine (**11d**)*

Yield: 46.47%, yellow solid, mp: 187.3–190.1 °C. Purity 98.91% by HPLC. ^{1}H NMR (400 MHz, $CDCl_3$) δ: 0.95 (d, 3H, J = 5.5 Hz, CH_3), 1.40 (m, 2H, H-3‴$_{ax}$ and H-5‴$_{ax}$), 1.41 (m, 1H, CH), 1.67 (d, 2H, J = 10.3 Hz, H-3‴$_{eq}$ and H-5‴$_{eq}$), 2.10 (t, 2H, J = 11.1 Hz, H-2‴$_{ax}$ and 6‴$_{ax}$), 2.18 (m, 2H, CH_2**CH_2**CH_2), 2.36 (s, 3H, $ArCH_3$), 2.65 (t, 2H, J = 7.6 Hz, NCH_2), 3.03 (d, 2H, J = 11.1 Hz, H-2‴$_{eq}$ and H-6‴$_{eq}$), 3.32

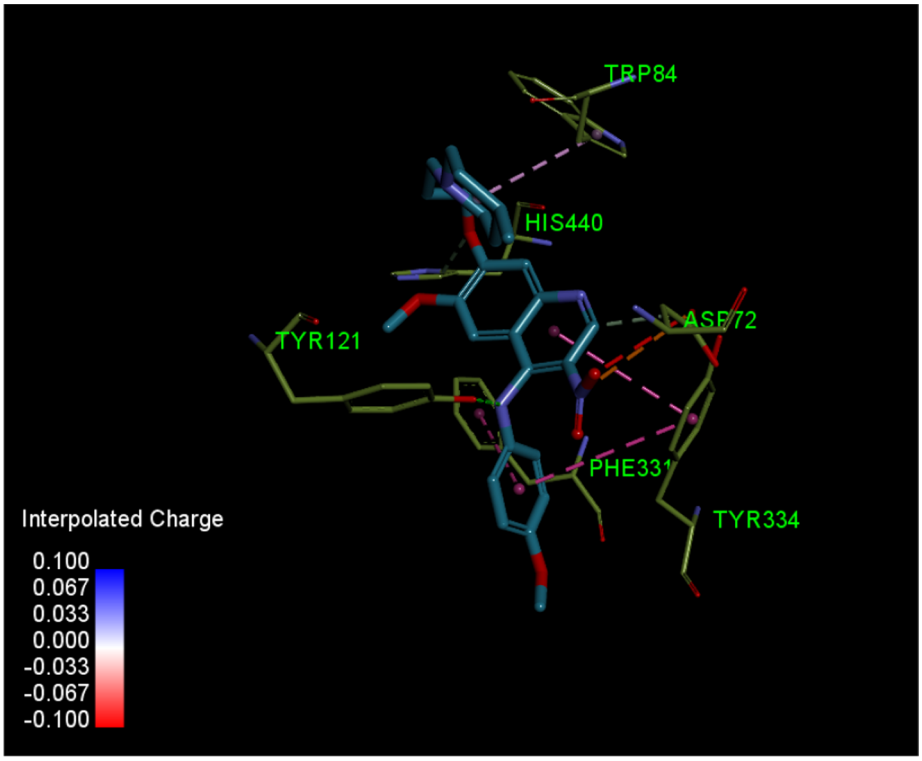

Fig. 7. 3D binding mode of compound **11j** with AChE (PDB code: 1DX6), highlighting the protein residues that participate in the main interactions with the inhibitor.

(s, 3H, OCH_3), 4.22 (t, J = 6.4 Hz, 2H, OCH_2), 6.87 (s, 1H, H-5), 7.08 (d, 2H, J = 8.1 Hz, H-3′, H-5′), 7.20 (d, 2H, J = 8.1 Hz, H-2′, H-6′), 7.30 (s, 1H, H-8), 9.32 (s, 1H, H-2), 10.45 (s, 1H, NH); ^{13}C NMR (100 MHz, $CDCl_3$) δ: 153.3, 148.0, 147.9, 145.5, 145.4, 138.5, 136.1, 130.2 (2C), 128.0, 124.3 (2C), 112.6, 109.9, 106.5, 67.4, 55.2, 55.1, 53.8 (2C), 33.5 (2C), 30.4, 25.9, 21.7, 21.0. HRMS (ESI) calculated for ($C_{26}H_{32}N_4O_4$ + H^+) 465.2502, found 465.2506.

*4.1.6. 6-Methoxy-7-(3-(4-methylpiperidin-1-yl)propoxy)-3-nitro-N-(2-chlorophenyl)quinolin-4-amine **(11e)***

Yield: 44.97%, yellow solid, mp: 135.4–137.7 °C. Purity 98.85% by HPLC. ^{1}H NMR (400 MHz, $CDCl_3$) δ: 0.92 (d, 3H, J = 6.4 Hz, CH_3), 1.25 (m, 2H, H-3′″$_{ax}$ and H-5′″$_{ax}$), 1.35 (m, 1H, CH), 1.62 (d, 2H, J = 12.1 Hz, H-3′″$_{eq}$ and H-5′″$_{eq}$), 1.93 (t, 2H, J = 11.4 Hz, H-2′″$_{ax}$ and 6′″$_{ax}$), 2.10 (m, 2H, CH_2**CH_2**CH_2), 2.51 (t, 2H, J = 7.1 Hz, NCH_2), 2.90

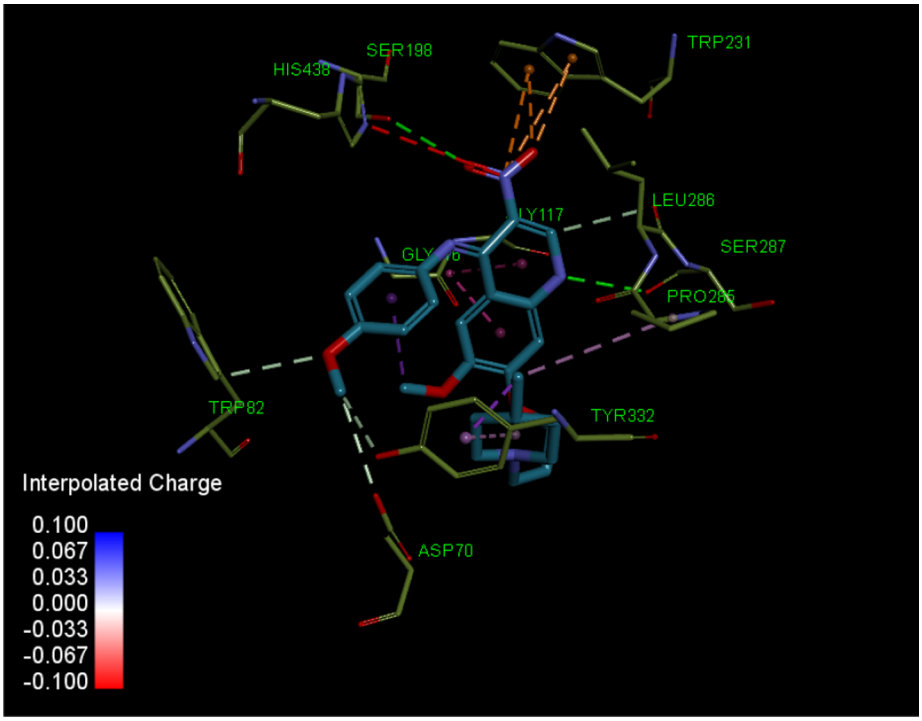

Fig. 8. 3D binding mode of compound **11j** with BChE (PDB code: 4BDS), highlighting the protein residues that participate in the main interactions with the inhibitor.

(d, 2H, J = 11.4 Hz, H-2‴$_{eq}$ and H-6‴$_{eq}$), 3.41 (s, 3H, OCH_3), 4.24 (t, 2H, J = 6.7 Hz, OCH_2), 6.75 (s, 1H, H-5), 6.97 (dd, 1H, J = 7.5 Hz, 1.8 Hz, H-6′), 7.18 (m, 2H, H-4′, H-5′), 7.37 (s, 1H, H-8), 7.54 (dd, 1H, J = 7.6, 1.7 Hz, H-3′), 9.35 (s, 1H, H-2), 10.14 (s, 1H, NH); ^{13}C NMR (100 MHz, $CDCl_3$) δ: 154.0, 148.9, 148.0, 145.0, 143.9, 138.4, 130.5, 129.5, 128.0, 127.4, 126.3, 124.4, 113.0, 109.9, 105.2, 67.9, 55.4, 55.3, 54.1 (2C), 34.4 (2C), 30.8, 26.5, 21.9. HRMS (ESI) calculated for ($C_{25}H_{29}ClN_4O_4$ + H^+) 485.1956, found 485.1956.

4.1.7. 6-Methoxy-7-(3-(4-methylpiperidin-1-yl)propoxy)-3-nitro-N-(3-chlorophenyl)quinolin-4-amine (**11f**)

Yield: 43.49%, yellow solid, mp: 154.3–155.8 °C. Purity 96.83% by HPLC. ^{1}H NMR (400 MHz, $CDCl_3$) δ: 0.92 (d, 3H, J = 6.3 Hz, CH_3), 1.26 (m, 2H, H-3‴‴$_{ax}$ and H-5‴$_{ax}$), 1.35 (m, 1H, CH), 1.63 (d, 2H, J = 12.7 Hz, H-3‴$_{eq}$ and H-5‴$_{eq}$), 1.94 (t, 2H, J = 11.4 Hz, H-2‴$_{ax}$ and 6‴$_{ax}$), 2.11 (m, 2H, CH_2**CH_2**CH_2), 2.52 (t, 2H, J = 7.1 Hz, NCH_2), 2.90 (d, 2H, J = 11.4 Hz, H-2‴$_{eq}$ and H-6‴$_{eq}$), 3.44 (s, 3H, OCH_3), 4.24 (t, 2H, J = 6.7 Hz, OCH_2), 6.83 (s, 1H, H-5), 7.01 (d, 1H, J = 8.0 Hz, H-6′), 7.15 (s, 1H, H-2′), 7.19 (d, 1H, J = 8.1, H-4′), 7.30 (t, J = 8.0 Hz, 1H, H-5′), 7.37 (s, 1H, H-8), 9.34 (s, 1H, H-2), 10.19 (s, 1H, NH); ^{13}C NMR (100 MHz, $CDCl_3$) δ: 154.0, 148.8, 148.2, 145.0, 143.8, 142.5, 135.3, 130.5, 129.3, 125.5, 123.2, 121.2, 112.7, 110.0, 105.8, 67.9, 55.4, 55.3, 54.1, 34.3, 30.8, 26.5, 21.9. HRMS (ESI) calculated for ($C_{25}H_{29}ClN_4O_4$ + H^+) 485.1956, found 485.1950.

4.1.8. 6-Methoxy-7-(3-(4-methylpiperidin-1-yl)propoxy)-3-nitro-N-(4-chlorophenyl)quinolin-4-amine (**11g**)

Yield: 44.26%, yellow solid, mp: 219.8–220.9 °C. Purity 97.49% by HPLC. ^{1}H NMR (400 MHz, $CDCl_3$) δ: 0.93 (d, 3H, J = 6.3 Hz, CH_3), 1.26 (m, 2H, H-3‴$_{ax}$ and H-5‴$_{ax}$), 1.36 (m, 1H, CH), 1.63 (d, 2H, J = 12.8 Hz, H-3‴$_{eq}$ and H-5‴$_{eq}$), 1.94 (t, 2H, J = 11.4 Hz, H-2‴$_{ax}$ and 6‴$_{ax}$), 2.10 (m, 2H, CH_2**CH_2**CH_2), 2.52 (t, 2H, J = 7.1 Hz, NCH_2), 2.90 (d, 2H, J = 11.4 Hz, H-2‴$_{eq}$ and H-6‴$_{eq}$), 3.43 (s, 3H, OCH_3), 4.24 (t, J = 6.6 Hz, 2H, OCH_2), 6.81 (s, 1H, H-5), 7.09 (d, 2H, J = 8.6 Hz, H-2′, H-6′), 7.35 (d, 2H, J = 7.6 Hz, H-3′, H-5′), 7.36 (s, 1H, H-8), 9.35 (s, 1H, H-2), 10.23 (s, 1H, NH); ^{13}C NMR (100 MHz, $CDCl_3$) δ δ: 153.9, 148.6, 148.2, 145.1, 144.3, 139.9, 131.0, 129.7 (2C), 129.0, 124.7 (2C), 112.6, 110.0, 105.9, 67.9, 55.34, 55.28, 54.1 (2C), 34.4 (2C), 30.8, 26.5, 21.9. HRMS (ESI) calculated for ($C_{25}H_{29}ClN_4O_4$ + H^+) 485.1956, found 485.1956.

4.1.9. 6-Methoxy-7-(3-(4-methylpiperidin-1-yl)propoxy)-3-nitro-N-(2-methoxyphenyl)quinolin-4-amine (**11h**)

Yield: 46.23%, yellow solid, mp: 103.2–105.7 °C. Purity 98.30% by HPLC. ^{1}H NMR (400 MHz, $CDCl_3$) δ: 1.03 (d, 3H, J = 6.3 Hz, CH_3), 1.67–2.02 (m, 5H, H-3‴, H-4‴ and H-5‴ of piperidyl moiety), 2.56 (m, 2H, CH_2**CH_2**CH_2), 2.91 (br.s, 2H, H-2‴$_{ax}$ and 6‴$_{ax}$), 3.33 (t, 2H, J = 7.0 Hz, NCH_2), 3.34 (s, 3H, OCH_3), 3.63 (br.s, 2H, H-2‴$_{eq}$ and H-6‴$_{eq}$), 3.81 (s, 3H, OCH_3), 4.25 (t, 2H, J = 5.7 Hz, OCH_2), 6.923 (td, 1H, J = 7.8, 1.2 Hz, H-4′), 6.924 (s, 1H, H-5), 7.00 (dd,1H, J = 7.8, 1.2 Hz, H-6′), 7.03 (dd, 1H, J = 7.8, 1.2 Hz, H-3′), 7.21 (td, 1H, J = 7.8, 1.2 Hz, H-5′), 7.23 (s, 1H, H-8), 9.25 (s, 1H, H-2), 10.24 (s, 1H, NH); ^{13}C NMR (100 MHz, $CDCl_3$) δ: 152.6, 152.4, 147.9, 147.2, 145.3, 145.2, 129.4, 128.4, 126.9, 124.0, 120.7, 113.6, 111.7, 110.0, 105.7, 66.1, 55.9, 55.3, 55.2, 53.3 (2C), 30.7 (2C), 29.0, 27.7, 23.6. HRMS (ESI) calculated for ($C_{26}H_{32}N_4O_5$ + H^+) 481.2451, found 481.2463.

4.1.10. 6-Methoxy-7-(3-(4-methylpiperidin-1-yl)propoxy)-3-nitro-N-(3-methoxyphenyl)quinolin-4-amine (**11i**)

Yield: 45.23%, yellow solid, mp: 104.9–105.7 °C. Purity 96.93% by HPLC. ^{1}H NMR (400 MHz, $CDCl_3$) δ: 1.03 (d, 3H, J = 6.3 Hz, CH_3), 1.76 (m, 1H, CH), 1.88 (d, 2H, J = 13.6 Hz, H-3‴$_{eq}$ and H-5‴$_{eq}$), 2.02 (m, 2H, H-3‴$_{ax}$ and H-5‴$_{ax}$), 2.58 (m, 2H, CH_2**CH_2**CH_2), 2.88 (t, 2H, J = 10.7 Hz, H-2‴$_{ax}$ and 6‴$_{ax}$), 3.33 (br.s, 2H, NCH_2), 3.37 (s, 3H, OCH_3), 3.69 (d, 2H, J = 10.7 Hz, H-2‴$_{eq}$ and H-6‴$_{eq}$), 3.77 (s, 3H, OCH_3), 4.26 (br.s, 2H, OCH_2), 6.72 (m, 1H, H-6′), 6.74 (s, 1H, H-2′), 6.79 (dd, 1H, J = 8.2 Hz, 1.8 Hz, H-4′), 6.90 (s, 1H, H-5), 7.25 (s, 1H, H-8), 7.29 (t, 1H, J = 8.0 Hz, H-5′), 9.25 (s, 1H, H-2), 10.35 (s, 1H, NH); ^{13}C NMR (100 MHz, $CDCl_3$) δ: 160.8, 152.8, 148.0, 147.4, 145.1, 144.9, 142.0, 130.5, 128.5, 116.2, 113.3, 111.8, 109.9, 109.7, 106.6, 66.2, 55.6, 55.3, 53.2, 53.4 (2C), 30.7 (2C), 29.2, 23.6, 21.0. HRMS (ESI) calculated for ($C_{26}H_{32}N_4O_5$ + H^+) 481.2451, found 481.2444.

4.1.11. 6-Methoxy-7-(3-(4-methylpiperidin-1-yl)propoxy)-3-nitro-N-(4-methoxyphenyl)quinolin-4-amine (**11j**)

Yield: 47.11%, yellow solid, mp: 102.6–104.7 °C. Purity 99.77% by HPLC. ^{1}H NMR (400 MHz, $CDCl_3$) δ: 1.04 (d, 3H, J = 6.3 Hz, CH_3), 1.68–2.03 (m, 5H, H-3‴, H-4‴ and H-5‴ of piperidyl moiety), 2.56 (m, 2H, CH_2**CH_2**CH_2), 2.90 (br.s, 2H, H-2‴$_{ax}$ and 6‴$_{ax}$), 3.32 (t, 2H, J = 7.7 Hz, NCH_2), 3.33 (s, 3H, OCH_3), 3.64 (br.s, 2H, H-2‴$_{eq}$ and H-6‴$_{eq}$), 3.83 (s, 3H, OCH_3), 4.25 (t, J = 5.7 Hz, OCH_2), 6.89 (s, 1H, H-5), 6.94 (d, 2H, J = 8.8 Hz, H-2′, H-6′), 7.15 (d, J = 8.8 Hz, 2H, H-2′, H-5′), 7.21 (s, 1H, H-8), 9.24 (s, 1H, H-2), 10.49 (s, 1H, NH); ^{13}C NMR (100 MHz, $CDCl_3$) δ: 158.1, 152.5, 147.63, 147.56, 145.8, 145.4, 133.7, 127.6, 126.1 (2C), 115.0 (2C), 112.8, 110.1, 106.6, 66.2, 55.7, 55.2, 55.1, 53.3 (2C), 30.7 (2C), 29.0, 23.7, 20.9. HRMS (ESI) calculated for ($C_{26}H_{32}N_4O_5$ + H^+) 481.2451, found 481.2475.

4.1.12. 6-Methoxy-7-(3-(4-methylpiperidin-1-yl)propoxy)-3-nitro-N-(3-hydroxylphenyl)quinolin-4-amine (**11k**)

Yield: 46.20%, yellow solid, mp: 84.6–87.2 °C. Purity 97.90% by HPLC. ^{1}H NMR (400 MHz, $CDCl_3$) δ: 0.93 (d, 3H, J = 6.3 Hz, CH_3), 1.30 (m, 2H, H-3‴$_{ax}$ and H-5‴$_{ax}$), 1.38 (m, 1H, CH), 1.63 (d, 2H, J = 12.4 Hz, H-3‴$_{eq}$ and H-5‴$_{eq}$), 2.03 (m, 2H, H-2‴$_{ax}$ and 6‴$_{ax}$), 2.06 (m, 2H, CH_2**CH_2**CH_2), 2.55 (t, 2H, J = 7.1 Hz, NCH_2), 2.93 (d, 2H, J = 10.8 Hz, H-2‴$_{eq}$ and H-6‴$_{eq}$), 3.39 (s, 3H, OCH_3), 4.06 (t, 2H, J = 6.0 Hz, OCH_2), 6.38 (s, 1H, H-2′), 6.75 (d, 2H, J = 7.6 Hz, H-4′, H-6′), 6.91 (s, 1H, H-5), 7.10 (s, 1H, H-8), 7.27 (t, 1H, J = 7.6 Hz, H-5′), 9.23 (s, 1H, H-2), 10.27 (s, 1H, NH); ^{13}C NMR (100 MHz, $CDCl_3$) δ: 158.5, 153.7, 148.2, 147.0, 145.2, 144.8, 142.1, 130.9, 128.3, 114.8, 114.0, 112.8, 110.9, 108.6, 106.5, 67.4, 55.3, 55.2, 53.9 (2C), 33.7 (2C), 30.6, 26.0, 21.7. HRMS (ESI) calculated for ($C_{25}H_{30}N_4O_5$ + H^+) 467.2294, found 467.2294.

4.1.13. 6-Methoxy-7-(3-(4-methylpiperidin-1-yl)propoxy)-3-nitro-N-(4-hydroxylphenyl)quinolin-4-amine (**11l**)

Yield: 47.12%, brown solid, mp: 124.8–126.3 °C. Purity 96.70% by HPLC. ^{1}H NMR (400 MHz, $CDCl_3$) δ: 0.94 (d, 3H, J = 5.2 Hz, CH_3), 1.35 (m, 2H, H-3‴$_{ax}$ and H-5‴$_{ax}$), 1.43 (m, 1H, CH), 1.68 (d, 2H, J = 11.4 Hz, H-3‴$_{eq}$ and H-5‴$_{eq}$), 2.11 (m, 2H, CH_2**CH_2**CH_2), 2.09 (m, 2H, H-2‴$_{ax}$ and 6‴$_{ax}$), 2.59 (*t*-like, 2H, NCH_2), 3.04 (d, 2H, J = 10.0 Hz, H-2‴$_{eq}$ and H-6‴$_{eq}$), 3.29 (s, 3H, OCH_3), 4.11 (*t*-like, 2H, OCH_2), 6.87 (d, 2H, J = 7.4 Hz, H-2′, H-6′), 6.97 (s, 1H, H-5), 7.09 (d, J = 7.4 Hz, 2H, H-3′, H-5′), 7.25 (s, 1H, H-8), 9.31 (s, 1H, H-2), 10.65 (s, 1H, NH); ^{13}C NMR (100 MHz, DMSO-d_6) δ: 155.1, 152.5, 148.2, 146.5, 144.8, 143.3, 132.5, 127.8, 124.1 (2C), 115.8 (2C), 113.4, 109.6, 104.5, 66.6, 55.4, 54.1, 52.8 (2C), 32.7 (2C), 29.5, 25.1, 21.5. HRMS (ESI) calculated for ($C_{25}H_{30}N_4O_5$ + H^+) 467.2294, found 467.2299.

4.1.14. 6-Methoxy-7-(3-(4-methylpiperidin-1-yl)propoxy)-3-nitro-N-(3-(trifluoromethyl)phenyl)quinolin-4-amine (**11m**)

Yield: 56.79%, brown solid, mp:136.0–139.3 °C. Purity 97.97% by HPLC. ^{1}H NMR (400 MHz, $CDCl_3$) δ: 1.05 (d, 3H, J = 6.2 Hz, CH_3), 1.73–2.07 (m, 5H, H-3‴, H-4‴ and H-5‴ of piperidyl moiety), 2.60 (br.s, 2H, CH_2**CH_2**CH_2), 2.90 (br.s, 2H, H-2‴$_{ax}$ and 6‴$_{ax}$), 3.35 (*t*-like, 2H, NCH_2), 3.38 (s, 3H, OCH_3), 3.68 (br.s, 2H, H-2‴$_{eq}$ and H-6‴$_{eq}$), 4.29 (*t*-like, 2H, OCH_2), 6.77 (s, 1H, H-5), 7.29 (s, 1H, H-8), 7.31 (d, 1H, J = 7.7 Hz, H-4′), 7.39 (s, 1H, H-2′), 7.46 (d, 1H, J = 7.7 Hz, H-6′), 7.52 (t, 1H, J = 7.7 Hz, H-5′), 9.30 (s, 1H, H-2), 10.20 (s, 1H, NH); ^{13}C NMR (100 MHz, $CDCl_3$) δ: 153.1, 148.7, 145.0, 143.5, 141.8, 132.1 (q, J = 32.9 Hz), 130.3 (2C), 129.6, 126.1, 123.5 (q, J = 270.9 Hz), 121.9 (q, J = 4.2 Hz), 119.4 (q, J = 4.1 Hz), 113.4, 110.5, 105.8, 66.3, 55.3,

55.2, 53.4 (2C), 30.8 (2C), 29.0, 23.7, 21.1. HRMS (ESI) calculated for ($C_{26}H_{29}F_3N_4O_4$ + H^+) 519.2219, found 519.2224.

4.2. Biological evaluation

4.2.1. AChE and BChE inhibition assay

AChE and BChE inhibitory activities of compounds were determined by using modified Ellman's method [49]. AChE (EC 3.1.1.7, from electric eel), BChE (EC 3.1.1.8, from equine serum), 5,5′-dithiobis(2-nitrobenzoic acid) (DTNB), acetylthiocholine iodide (ATCI), and butyrylthiocholine iodide (BTCI) were purchased from Sigma-Aldrich. Compounds were dissolved in DMSO (10 mM). Reaction mixture contained 140 μL of 100 mM sodium phosphate buffer (pH 8.0), the enzyme solution (either 0.05 U/mL of AChE, 20 μL; or 0.05 U/mL of BChE, 20 μL), and test compound (20 μL). Assayed solutions of test compounds were pre-incubated with corresponding ChE at 25 °C for 15 min. The reaction was initiated by addition of 10 μL of 10 mM DTNB and 10 μL of 7.5 mM substrate (ATCI or BTCI). The activity was determined by measuring the increase in absorbance at 412 nm at 37 °C in 10 min intervals using microplate reader (BioTek Epoch). The percentage of inhibition was calculated from the measured data as follows: (Ac − Ai)/Ac × 100%, where Ai and Ac represent the change in the absorbance in the presence of inhibitor and without inhibitor, respectively.

4.2.2. In vitro propidium iodide displacement assay

150 μL of a 20 μM solution of the test compound or standard donepezil (from Sigma) was incubated with 5 units of *ee*AChE at 25 °C for 6 h in the 96-well plate. After incubation, 50 μL of 1 μM propidium iodide solution was added to make the final assay volume of 200 μL. After 10 min, the fluorescence intensity was observed at an excitation wavelength (λex) of 535 nm and an emission wavelength (λem) of 595 nm using a fluorescence plate reader. The percentage inhibition was calculated by following expression: 100 − (IF_i/IF_0 × 100), where IF_i and IF_0 are the fluorescence intensities with and without the test compounds, respectively. Each assay was repeated at three different times [50,51].

4.2.3. Enzyme kinetic analysis against AChE

In order to investigate the reversibility of the compounds (**11a**, **11j**, **11k**, **11l**) against AChE, the absorbance was measured at 412 nm after two minutes of incubation at 37 °C for different concentrations of the compounds (0.0–2.0 μM) and five different concentrations of AChE (0.025–0.10 U/mL). The resulting values were measured in triplicate for the velocity and enzyme concentration curves. The velocity (V) was calculated from the measured data as follows: V = (Ac − Ai)/2, where Ai and Ac represent the change in the absorbance in the presence of AChE and without AChE, respectively. All data were analyzed by OriginPro 8.

For estimates of the inhibition model and inhibition constant K_i, the rate of enzymatic reaction was obtained with different concentrations of compounds (0.0–2.0 μM) and at least five different concentrations of ATCI (3.75–15.00 mM). For each experiment, reaction was started by adding substrate and progress curves were recorded at 412 nm after two minutes of incubation at 37 °C. Next, double reciprocal plots (1/v *vs* 1/[s]) were made using the slopes of progress curves to obtain the type of inhibition. Slopes of these reciprocal plots were then drawn against the concentration of a compound in a related analysis, and K_i was determined as the intercept on the negative x axis [52]. All rate measurements were performed in triplicate and data analysis was performed with OriginPro 8.0.

4.2.4. DPPH radical scavenging activity

The antioxidant activity was determined by the DPPH radical scavenging assay. The mixture was incubated for 30 min in the dark. The absorbance of the resulting solution was measured at 517 nm. Different concentrations (0.03125–1 mg/mL) of the extract were tested. The control sample was a mixture of methanol and DPPH, and Vc was used as reference. Percentage of DPPH radical scavenging activity was obtained as (1 − As/Ac) × 100. As and Ac represent the absorbance of the sample and control, respectively [44], and then EC_{50} (effective concentration of a compound that decreases the initial concentration of DPPH by 50%) can be calculated.

4.2.5. Metal-chelating properties

All solutions used in metal-chelating study were prepared in methanol, and Fe^{2+}, Cu^{2+}, $Al^{3+}$and Zn^{2+} solutions were prepared from $FeCl_2$, $CuCl_2$, $AlCl_3$ and $ZnCl_2$ respectively. To study the metal binding ability, a mixture of test compound (1 mL) and metal solution (1 mL) with the same concentration (20 μM) in a 1 cm quartz cuvette was incubated at room temperature for 30 min. Then, the absorption spectra were recorded with wavelength ranging from 200 to 600 nm [43].

The stoichiometry of complex **11l**-Cu^{2+} was also studied using the molar ratio method [4,53]. The concentration of tested compound **11l** was 20 μM and the final concentration of Cu^{2+} ranged from 0 to 60 μM at 282 nm. The plot was obtained by the corresponding absorption versus mole fraction of Cu^{2+}.

4.3. Docking study

4.3.1. Molecular docking studies on AChE

The binding modes were generated by using the Discovery Studio CDOCKER software (Accelrys, San Diego, USA). The crystal structure of AChE from Torpedo californica (*Tc*AChE; Code ID: 1DX6) was obtained from the Protein Data Bank. The binding pattern of galanthamine in *Tc*AChE is similar to that observed in human recombinant AChE (*rh*AChE) [54], hence *Tc*AChE was selected for docking studies [42,55]. *Tc*AChE was prepared for receptor protein by a sequence of operations including Clean Protein, Hydrogen Add and Apply Forcefield. All ligands were performed using the default settings, and docked in all possible stereoisomeric forms in an active site located sphere with 10 Å radius for *Tc*AChE. Then receptor-ligand interactions were operated by the CDOCKER protocol with the default parameters. By using the DS CDOCKER program, the crystallographic binding mode of galanthamine was reproduced into the *Tc*AChE binding site: the best ranked solution presented a root-mean-square deviations (RMSD) value of 0.50 Å with respect to the experimental pose, indicating that the docking methods and parameters used in this study were approximate for the AChE system.

4.3.2. Molecular docking studies on BChE

Flexible docking was conducted using Discovery Studio 2017 R2 (Accelrys, San Diego, USA). The crystal structure of BChE from Homo sapiens (Code ID: 4BDS) was extracted from the Protein Data Bank. And all water molecules and co-crystallized ligand were removed, which was followed by protein preparation protocol with CHARMm force field. The prepared ligands were subjected to minimization also with CHARMm force field before being used for docking analyses. The docking results were analyzed using Discovery Studio Visualizer 17.2.0.16349. The docking parameters were first validated by re-docking of cocrystallized ligand into the active site of the enzyme. The re-docked tacrine was found to bind in a similar manner as its respective crystallographic conformation, and the RMSD value for tacrine conformation is 0.41 Å, indicating that the selected docking parameters are acceptable.

Declaration of Competing Interest

The authors declare that they have no known competing financial interests or personal relationships that could have appeared to influence the work reported in this paper.

Acknowledgement

This research was supported by the Training Project of Innovation Team of Colleges and Universities in Tianjin (TD13-5020).

References

[1] Z. Cheng, J. Song, K. Zhu, J. Zhang, C. Jiang, H. Zhang, Total synthesis of pulmonarin B and design of brominated phenylacetic acid/tacrine hybrids: marine pharmacophore inspired discovery of new ChE and Aβ aggregation inhibitors, Mar. Drugs 16 (2018) 293.
[2] Q. He, J. Liu, J. Lan, J. Ding, Y. Sun, Y. Fang, N. Jiang, Z. Yang, L. Sun, Y. Jin, S. Xie, Coumarin-dithiocarbamate hybrids as novel multitarget AChE and MAO-B inhibitors against Alzheimer's disease: design, synthesis and biological evaluation, Bioorg. Chem. 81 (2018) 512–528.
[3] R.H. Swerdlow, Pathogenesis of Alzheimer's disease, Clin. Interv. Aging 2 (2007) 347–359.
[4] A. Rastegari, H. Nadri, M. Mahdavi, A. Moradi, S.S. Mirfazli, N. Edraki, F.H. Moghadam, B. Larijani, T. Akbarzadeh, M. Saeedi, Design, synthesis and anti-Alzheimer's activity of novel 1,2,3-triazole-chromenone carboxamide derivatives, Bioorg. Chem. 83 (2019) 391–401.
[5] K. Lodarski, J. Jonczyk, N. Guzior, M. Bajda, J. Gladysz, J. Walczyk, M. Jelen, B. Morak-Mlodawska, K. Pluta, B. Malawska, Discovery of butyrylcholinesterase inhibitors among derivatives of azaphenothiazines, J. Enzyme Inhib. Med. Chem. 30 (2015) 98–106.
[6] P. Sharma, P. Srivastava, A. Seth, P.N. Tripathi, A.G. Banerjee, S.K. Shrivastava, Comprehensive review of mechanisms of pathogenesis involved in Alzheimer's disease and potential therapeutic strategies, Prog. Neurobiol. 174 (2019) 53–89.
[7] S. Kocahan, Z. Doğan, Mechanisms of Alzheimer's disease pathogenesis and prevention: The brain, neural pathology, N-methyl-D-aspartate receptors, tau protein and other risk factors, Clin. Psychopharm. Neu. 15 (2017) 1–8.
[8] J. Wang, W. Li, J. Qin, L. Wang, S. Wei, H. Tang, Assessment of novel azaanthraquinone derivatives as potent multi-target inhibitors of inflammation and amyloid-β aggregation in Alzheimer's disease, Bioorg. Chem. 83 (2019) 477–486.
[9] S.K. Shrivastava, S.K. Sinha, P. Srivastava, P.N. Tripathi, P. Sharma, M.K. Tripathi, A. Tripathi, P.K. Choubey, D.K. Waiker, L.M. Aggarwal, M. Dixit, S.C. Kheruka, S. Gambhir, S. Shankar, R.K. Srivastava, Design and development of novel p-aminobenzoic acid derivatives as potential cholinesterase inhibitors for the treatment of Alzheimer's disease, Bioorg. Chem. 82 (2019) 211–223.
[10] E.K. Olsen, E. Hansen, L.W.K. Moodie, J. Isaksson, K. Sepčić, M. Cergolj, J. Svenson, J.H. Andersen, Marine AChE inhibitors isolated from Geodia barretti: natural compounds and their synthetic analogs, Org. Biomol. Chem. 14 (2016) 1629–1640.
[11] S.F. McHardy, H.L. Wang, S.V. McCowen, M.C. Valdez, Recent advances in acetylcholinesterase inhibitors and reactivators: an update on the patent literature (2012–2015), Expert Opin. Ther. Pat. 27 (2017) 455–476.
[12] D. Panek, T. Wichur, J. Godyń, A. Pasieka, B. Malawska, Advances toward multifunctional cholinesterase and β-amyloid aggregation inhibitors, Future Med. Chem. 9 (2017) 1835–1854.
[13] A.A. Shah, T.A. Dar, P.A. Dar, S.A. Ganie, M.A. Kamal, A current perspective on the inhibition of cholinesterase by natural and synthetic inhibitors, Curr. Drug Metab. 18 (2017) 96–111.
[14] Z. Cheng, K. Zhu, J. Zhang, J. Song, L.A. Muehlmann, C. Jiang, C. Liu, H. Zhang, Molecular-docking-guided design and synthesis of new IAA-tacrine hybrids as multifunctional AChE/BChE inhibitors, Bioorg. Chem. 83 (2019) 277–288.
[15] J. Zhang, C. Jiang, Synthesis and evaluation of coumarin/piperazine hybrids as acetylcholinesterase inhibitors, Med. Chem. Res. 27 (2018) 1717–1727.
[16] Y. Liu, L. Tian, D. Hu, J. Nie, Syntheses and anti-cholinesterase activity of 4-*N*-phenylaminoquinoline derivatives, Chem. J. Chin. Univ. 38 (2017) 392–397.
[17] E. Sawatzky, S. Wehle, B. Kling, J. Wendrich, G. Bringmann, C.A. Sotriffer, J. Heilmann, M. Decker, Discovery of highly selective and nanomolar carbamate-based butyrylcholinesterase inhibitors by rational investigation into their inhibition mode, J. Med. Chem. 59 (2016) 2067–2082.
[18] C.G. Ballard, Advances in the treatment of Alzheimer's disease: benefits of dual cholinesterase inhibition, Eur. Neurol. 47 (2002) 64–70.
[19] D.J. Lehmann, C. Johnston, A.D. Smith, Synergy between the genes for butyrylcholinesterase K variant and apolipoprotein E4 in late-onset confirmed Alzheimer's disease, Hum. Mol. Genet. 6 (1997) 1933–1936.
[20] D. Knez, N. Coquelle, A. Pišlar, S. Žakelj, M. Jukič, M. Sova, J. Mravljak, F. Nachon, X. Brazzolotto, J. Kos, J. Colletier, S. Gobec, Multi-target-directed ligands for treating Alzheimer's disease: butyrylcholinesterase inhibitors displaying antioxidant and neuroprotective activities, Eur. J. Med. Chem. 156 (2018) 598–617.
[21] B. Kumar, A.R. Dwivedi, B. Sarkar, S.K. Gupta, S. Krishnamurthy, A.K. Mantha, J. Parkash, V. Kumar, 4,6-diphenylpyrimidine derivatives as dual inhibitors of monoamine oxidase and acetylcholinesterase for the treatment of Alzheimer's disease, ACS Chem. Neurosci. 10 (2018) 252–265.
[22] N. Salehi, B.B.F. Mirjalili, H. Nadri, Z. Abdolahi, H. Forootanfar, A. Samzadeh-Kermani, T.T. Küçükkılınç, B. Ayazgok, S. Emami, I. Haririan, M. Sharifzadeh, A. Foroumadi, M. Khoobi, Synthesis and biological evaluation of new N-benzylpyridinium-based benzoheterocycles as potential anti-Alzheimer's agents, Bioorg. Chem. 83 (2019) 559–568.
[23] S.T. Tanoli, M. Ramzan, A. Hassan, A. Sadiq, M.S. Jan, F.A. Khan, F. Ullah, H. Ahmad, M. Bibi, T. Mahmood, U. Rashid, Design, synthesis and bioevaluation of tricyclic fused ring system as dual binding site acetylcholinesterase inhibitors, Bioorg. Chem. 83 (2019) 336–347.
[24] E. Yang, U. Mahmood, H. Kim, M. Choi, Y. Choi, J. Lee, J. Cho, J.W. Hyun, Y.S. Kim, M. Chang, H. Kim, Phloroglucinol ameliorates cognitive impairments by reducing the amyloid β peptide burden and pro-inflammatory cytokines in the hippocampus of 5XFAD mice, Free Radical Bio. Med. 126 (2018) 221–234.
[25] C. Rodríguez-Rodríguez, M. Telpoukhovskaia, C. Orvig, The art of building multifunctional metal-binding agents from basic molecular scaffolds for the potential application in neurodegenerative diseases, Coord. Chem. Rev. 256 (2012) 2308–2332.
[26] K.O. Yerdelen, E. Tosun, Synthesis, docking and biological evaluation of oxamide and fumaramide analogs as potential AChE and BuChE inhibitors, Med. Chem. Res. 24 (2015) 588–602.
[27] Y. Wang, Y. Yang, K.H. Hong, Y. Ning, P. Yu, J. Ren, M. Ji, J. Cai, Design, synthesis and evaluation of a novel metal chelator as multifunctional agents for the treatment of Alzheimer's disease, Bioorg. Chem. 87 (2019) 720–727.
[28] N. Miceli, E. Cavò, S. Ragusa, F. Cacciola, P. Dugo, L. Mondello, A. Marino, F. Cincotta, C. Condurso, M.F. Taviano, Phytochemical characterization and biological activities of a hydroalcoholic extract obtained from the aerial parts of *Matthiola incana* (L.) $R.B_R.$ subsp. *incana* (Brassicaceae) growing wild in Sicily (Italy), Chem. Biodivers. 16 (2019) e1800677.
[29] F. Prati, C. Bergamini, R. Fato, O. Soukup, J. Korabecny, V. Andrisano, M. Bartolini, M.L. Bolognesi, Novel 8-hydroxyquinoline derivatives as multitarget compounds for the treatment of Alzheimer's disease, ChemMedChem 11 (2016) 1284–1295.
[30] S.A. Nawaz, M. Ayaz, W. Brandt, L.A. Wessjohann, B. Westermann, Cation–π and π–π stacking interactions allow selective inhibition of butyrylcholinesterase by modified quinine and cinchonidine alkaloids, Biochem. Bioph. Res. Co. 404 (2011) 935–940.
[31] H. Boulebd, L. Ismaili, H. Martin, A. Bonet, M. Chioua, J.M. Contelles, A. Belfaitah, New (benz)imidazolopyridino tacrines as nonhepatotoxic, cholinesterase inhibitors for Alzheimer disease, Future Med. Chem. 9 (2017) 723–729.
[32] M. Go, T. Ngiam, L. Lim, Anticholinesterase activity of 4-aminoquinolines related to amodiaquine and their respective N-oxides, Eur. J. Med. Chem. 21 (1986) 81–85.
[33] Z. Najafi, M. Saeedi, M. Mahdavi, R. Sabourian, M. Khanavi, M.B. Tehrani, F.H. Moghadam, N. Edraki, E. Karimpor-Razkenari, M. Sharifzadeh, A. Foroumadi, A. Shafiee, T. Akbarzadeh, Design and synthesis of novel anti-Alzheimer's agents: acridine-chromenone and quinoline-chromenone hybrids, Bioorg. Chem. 67 (2016) 84–94.
[34] S.P. Mantoani, T.P.C. Chierrito, A.F.L. Vilela, C.L. Cardoso, A. Martínez, I. Carvalho, Novel triazole-quinoline derivatives as selective dual binding site acetylcholinesterase inhibitors, Molecules 21 (2016) 193.
[35] J. Zhu, L. Wang, R. Cai, S. Geng, Y. Dong, Y. Liu, Design, synthesis, evaluation and molecular modeling study of 4-*N*-phenylaminoquinolines for Alzheimer disease treatment, Bioorg. Med. Chem. Lett. 29 (2019) 1325–1329.
[36] X. Gao, C. Zhou, H. Liu, L. Liu, J. Tang, X. Xia, Tertiary amine derivatives of chlorochalcone as acetylcholinesterase (AChE) and butylcholinesterase (BuChE) inhibitors: the influence of chlorine, alkyl amine side chain and α, β-unsaturated ketone group, J. Enzyme Inhib. Med. Chem. 32 (2017) 146–152.
[37] H. Liu, L. Liu, X. Gao, Y. Liu, W. Xu, W. He, H. Jiang, J. Tang, H. Fan, X. Xia, Novel ferulic amide derivatives with tertiary amine side chain as acetylcholinesterase and butyrylcholinesterase inhibitors: the influence of carbon spacer length, alkylamine and aromatic group, Eur. J. Med. Chem. 126 (2017) 810–822.
[38] F. Mehrabi, Y. Pourshojaei, A. Moradi, M. Sharifzadeh, L. Khosravani, R. Sabourian, S. Rahmani-Nezhad, M. Mohammadi-Khanaposhtani, M. Mahdavi, A. Asadipour, H.R. Rahimi, S. Moghimi, A. Foroumadi, Design, synthesis, molecular modeling and anticholinesterase activity of benzylidenebenzofuran-3-ones containing cyclic amine side chain, Future Med. Chem. 9 (2017) 659–671.
[39] P. Sharma, A. Tripathi, P.N. Tripathi, S.K. Prajapati, A. Seth, M.K. Tripathi, P. Srivastava, V. Tiwari, S. Krishnamurthy, S.K. Shrivastava, Design and development of multitarget-directed N-Benzylpiperidine analogs as potential candidates for the treatment of Alzheimer's disease, Eur. J. Med. Chem. 167 (2019) 510–524.
[40] P. Meena, V. Nemaysh, M. Khatri, A. Manral, P.M. Luthra, M. Tiwari, Synthesis, biological evaluation and molecular docking study of novel piperidine and piperazine derivatives as multi-targeted agents to treat Alzheimer's disease, Bioorg. Med. Chem. 23 (2015) 1135–1148.
[41] U. Košak, D. Knez, N. Coquelle, B. Brus, A. Pišlar, F. Nachon, X. Brazzolotto, J. Kos, J. Colletier, S. Gobec, N-propargylpiperidines with naphthalene-2-carboxamide or naphthalene-2-sulfonamide moieties: potential multifunctional anti-Alzheimer's agents, Bioorg. Med. Chem. 25 (2017) 633–645.
[42] Y. Liu, Y. Feng, X. Lu, J. Nie, W. Li, L. Wang, L. Tian, Q. Liu, Isosteroidal alkaloids as potent dual-binding site inhibitors of both acetylcholinesterase and butyrylcholinesterase from the bulbs of *Fritillaria walujewii*, Eur. J. Med. Chem. 137 (2017) 280–291.
[43] M. Mahdavi, R. Hariri, S.S. Mirfazli, H. Lotfian, A. Rastergari, O. Firuzi, N. Edraki, B. Larijani, T. Akbarzadeh, M. Saeedi, Synthesis and biological activity of some benzochromenoquinolinones: tacrine analogs as potent anti-Alzheimer's agents, Chem. Biodivers. 16 (2019) e1800488.
[44] R. Spinelli, I. Sanchis, F.M. Aimaretti, A.M. Attademo, M. Portela, M.V. Humpola, G.G. Tonarelli, A.S. Siano, Natural multi-target inhibitors of cholinesterases and monoamine oxidase enzymes with antioxidant potential from skin extracts of *Hypsiboas cordobae* and *Pseudis minuta* (Anura: Hylidae), Chem. Biodivers. 16 (2019) e1800472.
[45] G.A. Berwaldt, D.P. Gouvea, D.S. da Silva, A.M. das Neves, M.S.P. Soares, J.H. zambuja, G.M. Siqueira, R.M. Spanevello, W. Cunico, Synthesis and biological evaluation of benzothiazin- 4-ones: a possible new class of acetylcholinesterase inhibitors, J. Enzyme Inhib. Med. Chem. 34 (2019) 197–203.
[46] Y. Chen, M. Wang, H. Fu, X. Qu, Z. Zhang, F. Kang, D. Zhu, Spectroscopic and molecular modeling investigation on inhibition effect of nitroaromatic compounds

on acetylcholinesterase activity, Chemosphere 236 (2019) 124365.
[47] D. Secci, S. Carradori, A. Petzer, P. Guglielmi, M. D'Ascenzio, P. Chimenti, D. Bagetta, S. Alcaro, G. Zengin, J.P. Petzer, F. Ortuso, 4-(3-Nitrophenyl)thiazol-2-ylhydrazone derivatives as antioxidants and selective hMAO-B inhibitors: synthesis, biological activity and computational analysis, J. Enzyme Inhib. Med. Chem. 34 (2019) 597–612.
[48] S. Gawaskar, D. Schepmann, A. Bonifazi, D. Robaa, W. Sippl, B. Wünsch, Benzo[7] annulene-based GluN2B selective NMDA receptor antagonists: surprising effect of a nitro group in 2-position, Bioorg. Med. Chem. Lett. 25 (2015) 5748–5751.
[49] G.L. Ellman, K.D. Courtney, V. Andres, R.M. Featherstone, A new and rapid colorimetric determination of acetylcholinesterase activity, Biochem. Pharmacol. 7 (1961) 88–95.
[50] P. Taylor, S. Lappi, Interaction of fluorescence probes with acetylcholinesterase, The Site Specif. Propid. Bind. Biochem. 14 (1975) 1989–1997.
[51] P.N. Tripathi, P. Srivastava, P. Sharma, M.K. Tripathi, A. Seth, A. Tripathi, S.N. Rai, S.P. Singh, S.K. Shrivastava, Biphenyl-3-oxo-1,2,4-triazine linked piperazine derivatives as potential cholinesterase inhibitors with anti-oxidant property to improve the learning and memory, Bioorg. Chem. 85 (2019) 82–96.
[52] A. Bosak, D.M. Opsenica, G. Šinko, M. Zlatar, Z. Kovarik, Structural aspects of 4-aminoquinolines as reversible inhibitors of human acetylcholinesterase and butyrylcholinesterase, Chem.-Biol. Interact. 308 (2019) 101–109.
[53] X. Zhang, Q. Song, Z. Cao, Y. Li, C. Tian, Z. Yang, H. Zhang, Y. Deng, Design, synthesis and evaluation of chalcone mannich base derivatives as multifunctional agents for the potential treatment of Alzheimer's disease, Bioorg. Chem. 87 (2019) 395–408.
[54] J. Cheung, M.J. Rudolph, F. Burshteyn, M.S. Cassidy, E.N. Gary, J. Love, M.C. Franklin, J.J. Height, Structures of human acetylcholinesterase in complex with pharmacologically important ligands, J. Med. Chem. 55 (2012) 10282–10286.
[55] X. Yan, J. Tang, C.S. Passos, A. Nurisso, C.A. Simões-Pires, M. Ji, H. Lou, P. Fan, Characterization of lignanamides from hemp (*Cannabis sativa* l.) seed and their antioxidant and acetylcholinesterase inhibitory activities, J. Agric. Food Chem. 63 (2015) 10611–10619.